TITLE:

Behaviours of Bubbles in the Gas-Solid Fluidized-Beds

AUTHOR(S):

TOEI, Ryozo; MATSUNO, Ryuichi; KOJIMA, Hiroshi; NAGAI, Yoshiaki; NAKAGAWA, Koichi; YU, Shinichi

CITATION:

TOEI, Ryozo ...[et al]. Behaviours of Bubbles in the Gas-Solid Fluidized-Beds. Memoirs of the Faculty of Engineering, Kyoto University 1965, 27(4): 475-489

ISSUE DATE:

1965-12-10

URL:

http://hdl.handle.net/2433/280642

RIGHT:

京都大学学術情報リポジトリ
KURENAI 紅
Kyoto University Research Information Repository

Behaviours of Bubbles in the Gas-Solid Fluidized-Beds

By

Ryozo TOEI*, Ryuichi MATSUNO*, Hiroshi KOJIMA*, Yoshiaki NAGAI*, Koichi NAKAGAWA* and Shinichi YU*

(Received June 30, 1965)

The size, shape and rising velocity of bubbles and also particle concentration in bubbles which appeared in the air-solid fluidized bed were investigated by photography, X-ray photograpy, X-ray cinematography and capacitance method. The results were that the bubbles had nearly the shape of spherical cap and there were few particles in the bubbles.

Although the rising velocity of the bubble was affected largely by other bubbles, it was proportional to the square root of the vertical bubble length and the bubbles became large with the process of repetition of coalescence and redispersion.

Introduction

There were many studies about the operations such as reaction and heat transfer etc. in the gas-solid fluidized bed, and the mechanism of them was gradually made clear.

The most important suggestions of these studies were that we could not clearly understand the mechanism without studying the behaviours of bubbles which appeared in the gas-solid fluidized bed.

In fact, there were many researches with the object of studying the behaviours of bubbles by Yasui et al.,[23] Lanneau,[11] Baumgarten et al.,[1] Ozaki et al.,[14] Davidson et al.,[2] Harrison et al.,[7] Rowe et al.,[17,18,19,20,21] and Reuter.[15,16]

The authors carried out the studies about the behaviours of the bubbles also.

The experiments performed were tabulated in **Table 1.**

1. Experimental Procedures

Schematic diagram of experimental apparatus was showed in **Fig. 1. a,** The air was used as fluidizing fluid.

* Department of Chemical Engineering

Table 1. Experimental apparatuses, measuring methods and purposes.

Apparatus		Measuring method	Purpose
3 dimensional fluidized bed	$3''\phi \times 800^{H}$	electric capacitance method	rising velocity, size and frequency of continuous bubble
	$100 \times 100 \times 1000^{H}$	electric capacitance method	rising velocity and size of single and continuous bubble
		X-ray photography	shape and size of continuous bubble
		X-ray cinematography	shape, rising velocity and size of single and continuous bubble
2 dimensional fluidized bed $250^{W} \times 24^{T} \times 1500^{H}$		photography	shape of bubble concentration of particels in bubble (tomography) change of state of bubble by inserted probe
		electric capacitance method	calibration of electric capacitance method

1.1. Three dimensional fluidized bed

1.1.1. Apparatus of cylindrical fluidized bed and capacitometer—The rising velocity and vertical length of bubbles which generated spontaneously (continuous bubble) were investigated by capacitance method.

A cylinder 3 in. inside diameter and 800 mm height made of transparent and rigid polyvinyl-chloride was used as column.

The calming section was composed of fixed bed of filling 3 mm diameter lead shots up 15 cm height and a coarse and 200 mesh screen upon the fixed bed for reinforcement.

In this column, a probe measuring electric capacitance which was shown in **Fig. 1. b.** was installed every 5 centimeters to the longitudinal direction.

The change of electrical capacitance was occured when bubbles passed through the probe inserted in the fluidized bed and was recorded by a pen-oscillograph.

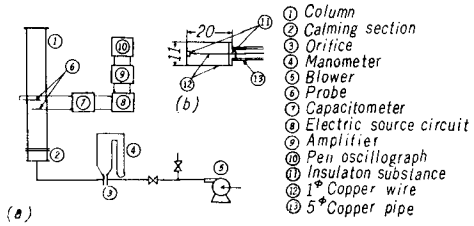

Fig. 1. (a) Schematic diagram of experimental apparatus by capacitance method. (b) Probe for capacitance method.

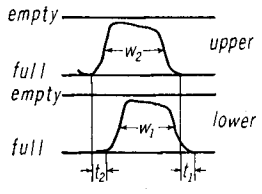

Fig. 2. Traces of pen-oscillograph.

This method was used widely.[5,11,13] The schematic diagram was shown in **Fig. 1. a.** So as not to obstruct the fluidized bed the probe was made of copper wire of 1 mm diameter.

An example of record of pen-oscillograph when gas bubbles passed through the probe was shown in **Fig. 2.**

As the interval of probe was 5 cm and a chart speed of pen-oscillograph was 125 mm/sec, the rising velocity of bubble u_b was calculated by Eq. (1).

$$u_b = \frac{125 \times 5}{(t_1 + t_2)/2} \tag{1}$$

And then the vertical length of bubble y was;

$$y = (w_1 + w_2) \times 5/(t_1 + t_2) \tag{2}$$

The values of w_1 and w_2 were taken as those at the position of half of the peaks on the chart. This was decided from the experiments performed at the same time by the capacitance method and photography in the two dimensional fluidized bed.

1. 1. 2. Apparatus of rectangular fluidized-bed and equipment for X-ray photography—A rectangular column 100 mm × 100 mm cross section and 1,000 mm height made of transparent and rigid polyvinyl-chloride was used.

A cintered metal of 1.5 cm thickness which was made of 100 μ alumina particles was used as a gas distributor. With this column, experiments listed up in Table 1 were performed. For the capacitance method, the probe was installed every 5 centimeters in the longitudinal direction. A nozzle to blow a bubble (a single bubble) was installed close to the bottom of the column. The X-ray photography and X-ray cinematography were performed also. These methods were used for the purpose of investigating the behaviours of bubbles which rose freely in the three dimensional fluidized bed without obstruction such as a probe.

A condenser method of 15×10^4 Volt was used for X-ray photography. Medical X-ray film (11 in. × 14 in.) was fixed close to the back of the column and X-ray

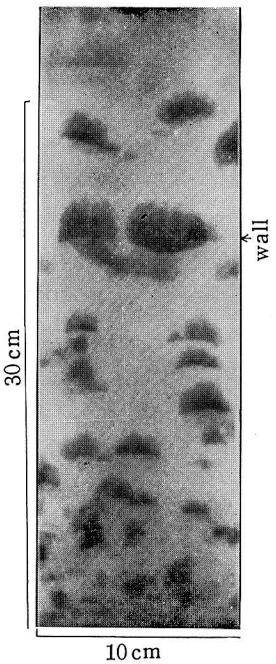

Fig. 3. Behaviours of bubbles in the three dimensional fluidized bed by X-ray photography.

was applied $\frac{2}{1000}\sim\frac{3}{1000}$ second from X-ray source which was 1~1.5 m away from film to the front of the column. The image of almost actual size was taken upon the film. An example of it was shown in **Fig. 3.**

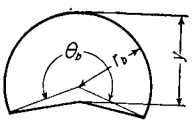

Fig. 4. Model of bubble.

From Fig. 3, it could be concluded that the bubbles had the shape of spherical cap and its lower part was convex upward, and could be shown as **Fig. 4.** The vertical length of bubble y, radius of bubble r_b and angle of bubble θ_b were measured. The distinguishable smallest size of bubble on the X-ray film was 2.5~3 mm.

The usual equipment of fluorescopy was used as the equipment of X-ray cinematography. The X-ray source was set 40 cm apart from the column and the fluorescent screen 7 cm apart from the back of it. The brightness of image on the fluorescent screen was amplified 200~300 times by image amplifier and the photographs were taken by 16 mm cine-camera. X-ray source was $11\times10^4\sim13\times10^4$ Volt, 3 milliamp. and 16 mm cine-camera was set 48 frame/sec, f : 1.4. The range of vision was the circle of about 8 cm diameter.

1.2. Apparatus of two dimensional fluidized bed and equipment of tomography

The column was 250 mm width, 25 mm thickness and 1,500 mm height and made of transparent and rigid polyvinyl-chloride. The probe for capacitance method could be installed. A nozzle to blow a bubble was installed close to the bottom of the column. Photographs were taken with the camera having the lens of the focal distance 50 mm to investigate the shape of bubble and the effect of the probe inserted in the fluidized bed upon the movement of bubbles and particles. The tomography of the inside of the bubble was carried out with this column to investigate how many particles were contained in the bubble. The camera for tomography was composed of the lens of focal distnce 50 mm, f : 3.5 and a dark box.

The range of vision was $3\times5\,cm^2$ and the image was magnified 4.2 times upon film. Images of particles (dia. 16~24#) disappeared at the plane of 5.5 mm apart from the focusing plane. As shown in **Fig. 5,** the focusing planes were set at ①, ②, ③, ④, ⑤ in the direction of thickness and the photographs were

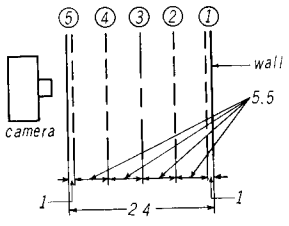

Fig. 5. Positions of planes pictured by tomography in the two dimensional fluidized bed.

taken when the bubble passed through. An example of the results was shown in **Fig. 6.** The fraction of the particles in the bubble was expressed as $(1-\varepsilon)$ at each plane ①, ②, ③, ④, ⑤. The volume of particles in the bubble was obtained by counting the number of particles which was taken on photograph and multiplying it by the volume of particle of average size, and the volume of space was obtained by multiplying the area of range of vision by 11 mm (at the planes of ① and ⑤ 6.5 mm was used). Then $(1-\varepsilon)$ was obtained by dividing the former by the latter.

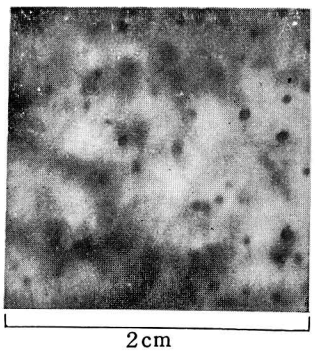

Fig. 6. Particles dispersed in the bubble pictured by tomography.

2. Results and Considerations

Testing particles being used were glass beads 80～100# (G.B. 1), glass beads 16～24# (G.B. 2), sand 80～120# (s. 1), sand 35～48# (s. 2) and polyvinyl-chloride powder 80～100# (B. 1).

2.1. Vertical length and frequency of bubble in three dimensional fluidized bed

Testing materials and experimental conditions were shown in **Table 2.** Relations between average vertical length of bubbles and the height from

Table 2. Experimental conditions in the section 2.1.

column dimension	measuring method	particles		symbol	u/u_{mf} [−]	Z_c [cm]
3 in, diameter	capacitance	glass beads	80–100#	G.B.1	1.83–1.07	20.7
	capacitance	glass beads	16–20#	G.B.2	1.55–4.4	20.7
	capacitance	sand	80–120#	s.1	1.45–10.6	20.7
100×100 rectangular	capacitance	glass beads	80–1000#	G.B.1	1.2–4.0	50.0
	X-ray photo.	glass beads	80–100#	G.B.1	1.2–4.0	50.0
	X-ray photo.	vinyl chloride	80–100#	B.1	1.2–4.0	50.0

distributor were shown in **Fig. 7, 8, 9** taking the flow rate as parameter. Fig. 7 was the results of glass beads 80～100# with capacitance method in 3 in. diameter column, Fig. 8, of glass beads 80～100# with capacitance method in 100 mm×100 mm column and Fig. 9, of glass beads 80～100# with X-ray photography in 100 mm×100 mm column. The value of $\bar{y}$ became larger as Z. It was considered that the bubbles became large with the process of repetition

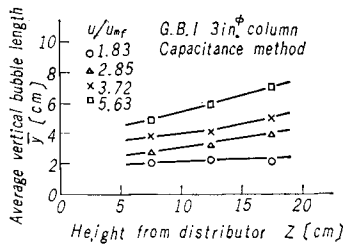

Fig. 7. Vertical bubble length.

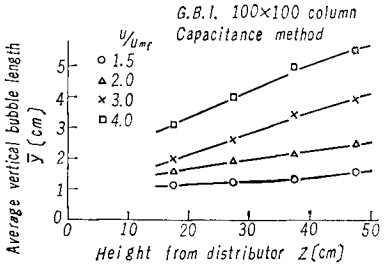

Fig. 8. Vertical bubble length.

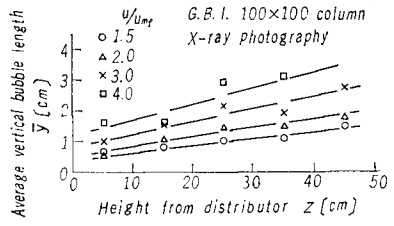

Fig. 9. Vertical bubble length.

of coalescence and redispersion caused by "finger".[20] The coalescence of bubbles could be observed on the chart of pen-oscillograph. Fig. 7 showed larger values of $\bar{y}$ than Fig. 8 for the same u/u_{mf}. The reason was considered as the difference of distributor which was mentioned in the section of experimental apparatus. The straightening of air stream by the calming section in the case of Fig. 7 was worse compared with that of Fig. 8 and then the larger values of $\bar{y}$ might be obtained. And as compared Fig. 8 with Fig. 9., Fig. 8 showed larger values of $\bar{y}$ than Fig. 9. It might be concluded that the lower limit of vertical length of bubble which could be detected by capacitometer was about 0.8 cm, so only the larger bubbles were detected by this method than X-ray photography.

Whether the bubble passed through the probe or through the side of it, the probe was affected by the motions of particles, so the capacitometer could detect the passing of bubbles. Then the total frequency of bubbles n [no./sec] which passed through the sectional area was obtained by counting the peaks which were recorded on the chart of pen-oscillograph. The total frequency of bubble in the 3 in. diameter fluidized bed had no relation with flow rate, and that the values of n were 6~7 at the height of 5 cm from distributor and decreased to 3~4 at the height of 20 cm. It indicated the existence of coalescence of bubbles. From this frequency and the bubble size mentioned above, the flow rates which flew as bubbles could be calculated, but the values of these differed enormusly from the results of Yasui et al.[23] which were carried out with light probe technique. Namely, the authors could not verified Yasui's results that the gas above minimum fluidization flow rate flew as bubbles. As with capacitance method, the accurate frequency could not be obtained when bubbles stood side by

side and very small bubble existed. As the measurement of frequency, therefore the flow rate flowing as bubbles was very important, this phenomena would be studied furthermore with other methods.

2.2. Shape of bubble

2.2.1. Shape of bubble in two dimensional fluidized bed—The photography was carried out to investigate the shape of bubble with glass beads G.B. 1 and G.B. 2 in the two dimensional fluidized bed mentioned in section 1.2. The sectional area of bubble had the shape shown in Fig. 4 and the bubble was the cylinder penetrating through the thickness of the fluidized bed. The value of θ_b measured were 257 deg. in average of 66 bubbles. The values of θ_b given from photographs of bubbles by Rowe[17,18,19,20] and Reuter[15,16] were $\theta_b=265$ deg. and $\theta_b=227$ deg. respectively. The result of Rowe coincided fairly well with the results of the authors. Although the bubble shown by Reuter was two dimensional also, but it was the bubble which appeared at the wall in three dimensional fluidized bed and then the value of θ_b differed. The bubbles which appeared at the wall were shown on X-ray photograph of Fig. 3. Those bubbles were not divided into equal parts, and had the shape deformed a little towards the wall. The bubble shown by Reuter might be such a one.

2.2.2. Shape of bubble in three dimensional fluidized bed—The shape of bubble which generated in the three dimensional fluidized bed mentioned in section 1.1.2 was investigated. Glass beads G.B. 1 was fluidized at $u/u_{mf}=1.2\sim4.0$ and polyvinyl-chrolide powder B. 1 at $u/u_{mf}=1.2\sim4.0$. The X-ray photography and X-ray cinematography were carried out. The bubbles had the shape shown in Fig. 4. The average values of θ_b and y/r_b of many bubbles became $\theta_b=215°$, $y/r_b=1.14$ for G.B. 1 and $\theta_b=206°$, $y/r_b=1.08$ for B. 1. Though these values were scattered widely, frequency curves of θ_b and y/r_b had the steep peak at the average value. In the same manner for a single bubble which was taken by X-ray cinematography, $\theta_b=214°$ and $y/r_b=1.26$ were obtained for G.B. 1 and there were little differences between single and continous bubble. Effects of bubble size, particle size and flow rate on θ_b and y/r_b could not be found. The difference of θ_b of the bubble by the two dimensional, three dimensional and Reuter's fluidized bed respectively appeared and was caused by the fact that the motion of particles around the bubble and the gas streaming differed from each other. Harrison et al.[7] obtained $\theta_b=120°$ but it showed great difference in comparison with the authors' result.

When the bubble had the shape shown in Fig. 4, the volume of bubble was obtained by Eq. (3).

$$V_b = \pi r_b^3\left(\frac{2}{3} - \cos\frac{\theta_b}{2} + \frac{1}{3}\cos^3\frac{\theta_b}{2} - \frac{1}{3}\sin^2\frac{\theta_b}{2} + \frac{1}{3}\sin^2\frac{\theta_b}{2}\cos\frac{\theta_b}{2} + \frac{y}{3r_b}\sin^2\frac{\theta_b}{2}\right) \quad (3)$$

By substituting $\theta_b = 215°$ and $y/r_b = 1.14$ for testing material G.B. 1 in Eq. (3), the volume of bubble was shown as Eq. (4).

$$V_b = 2.0\, y^3 \quad (4)$$

This result coincided with Rowe's one. The results by Rowe were shown in Eq. (5).

$$V_b = (1-f_b)\frac{4}{3}\pi r_b^3, \qquad f_b = 0.25 \quad (5)$$

2.3. Rising velocity of bubble

2.3.1. Rising velocity of single bubble—Glass beads G.B. 1. and polyvinyl-chloride powder B. 1. were fluidized near the minimum fluidization velocity in rectangular column (10×10 cm). A single bubble was blown into it, and the rising velocity u_b and vertical length y of it were measured with capacitance method and X-ray cinematography (glass beads only). As same as Harrison et al.[7] applying the correction by Uno et al.[22] for wall effect to u_b, $u_{b\infty}$ could be obtained. To make this correction the frontal diameter was calculated from $y/r_b = 1.14$ for glass beads and $y/r_b = 1.08$ for polyvinylchloride powder in the case of capacitance method, and it was taken from photograph in the case of X-ray cinematography. The values of $u_{b\infty}$ were plotted versus y in **Fig. 10.** Though it scattered in the range of ±25%, $u_{b\infty}$ was proportional to $\sqrt{y}$. In spite of the differences of testing materials (glass beads and polyvinyl-chloride powder) and of measuring methods (capacitance method and X-ray cinematography) each average value of $u_{b\infty}/\sqrt{y}$ coincided very well (difference 3～4%). As all over average value $u_{b\infty}/\sqrt{y} = 25.9$ was obtained, and the general relation was deduced.

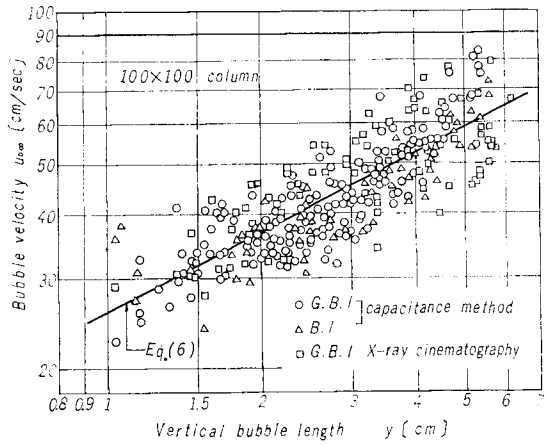

Fig. 10. Rising velocity of single bubble.

$$u_{b\infty} = 0.83\sqrt{gy} \tag{6}$$

Using the values of (y/r_b), θ_b and V_b, Eqs. (7), (8) were obtained.

$$u_{b\infty} = 0.74\sqrt{g}V_b^{1/6} \tag{7}$$

$$u_{b\infty} = 0.88\sqrt{gr_b} \tag{8}$$

Eq. (7) coincided well with the results by Harrison et al.[7] (Eq. (9)) and Davidson et al.[2] (Eq. (10)) also.

$$u_{b\infty} = 0.71\sqrt{g}V_b^{1/6} \tag{9}$$

$$u_{b\infty} = 0.792\sqrt{g}V_b^{1/6} \tag{10}$$

Eq. (8) showed larger value than Eq. (11) derived by Davies and Taylor,[4] and by Jackson,[8]

$$u_{b\infty} = \frac{2}{3}\sqrt{gr_b} \tag{11}$$

and larger value also than Eq. (12) obtained from the experimental results about the pressure distribution by Davies and Taylor.[4]

$$u_{b\infty} = 0.78\sqrt{gr_b} \tag{12}$$

2. 3. 2. Rising velocity of continuous bubble—The rising velocity of continuous bubble was measured by the capacitance method and X-ray cinematography. There were no differences by the kind of particles and the measuring method, but the difference by the dimension of the column was observed. It appeared as the wall effect. The rising velocity u_b in rectangular column (10×10 cm) was about 10% or more large than in 3 in. circular one on an average. As same as the single bubble, applying the correction by Uno et al. for wall effect, both results coincided. The relation between $u_{b\infty}$ and y was shown on **Fig. 11.** Though the scattering of data was very wide in comparison with the case of single bubble, average value of $u_{b\infty}/\sqrt{y}$ became 30.7 and

$$u_{b\infty} = 0.98\sqrt{gy} \tag{13}$$

was obtained,

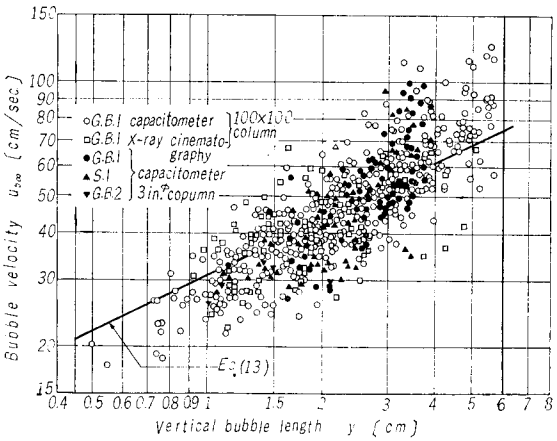

Fig. 11. Rising velocity of continuous bubble,

In comparison Fig. 10 with Fig. 11, the rising velocity of single bubble was smaller and was located at the lower part of the scattering of continuous bubble. Harrison and Davidson[3] described that the rising velocity of continuous bubble was equal to the rising velocity of single bubble plus $(u-u_{mf})$. The rising velocity $u_{b\infty}'$ was obtained by subtracting $(u-u_{mf})$ from rising velocity u_b and applying the correction by Uno et al. for wall effect. By this method, authors' data were calculated again and in spite of the differences of measuring method and of particles, the average value of $u_{b\infty}'/\sqrt{y}$ coincided each other within several %, and $u_{b\infty}'/\sqrt{y}=27.8$ was obtained. This value also was larger than velue of $u_{b\infty}/\sqrt{y}=25.9$ for single bubble and the scattering was large as before.

All above mentioned are listed up in **Table 3.**

Table 3. Comparison of result.

experimentor	particles	results
Rowe et al.[17,18,19,20,21]	ballotini 230μ etc.	2 dim.* $\theta_b=265°$ 3 dim.* $V_b=(1-f_b)\frac{4}{3}\pi r_b^3$ $f_b=0.25$
Reuter[15,16]	hartweizengrieß 0.2–0.3 mm quarz sand 0.5–1 mm	2 dim. $\theta_b=227°$
Davies et al.[4]	theoretical	3 dim. $u_{b\infty}=\frac{2}{3}\sqrt{gr_b}$
	air-water	3 dim. $u_{b\infty}=0.78\sqrt{gr_b}$
Jackson[8]	theoretical	3 dim. $u_{b\infty}=\frac{2}{3}\sqrt{gr_b}$
Davidson et al.[2]	glass beads 150μ sand 40–60# swede seeds 1.7 mm	3 dim. $\theta_b=100°$ $u_{b\infty}=0.792\sqrt{g}V_b^{1/6}$ single bubble
Harrison et al.[7]	sand 72–120#	3 dim. $\theta_b=120°$ $u_{b\infty}=0.71\sqrt{g}V_b^{1/6}$ single bubble
authors	G.B.1 G.B.2 G.B.1 G.B.2	2 dim. $\theta_b=257°$ 3 dim. $\theta_b=215°$, $y/r_b=1.14$ (glass beads) $V_b=2.0y^3$ $u_{b\infty}=0.83\sqrt{gy}=0.88\sqrt{gr_b}$ $u_{b\infty}=0.74\sqrt{g}V_b^{1/6}$ single bubble $u_{b\infty}=0.98\sqrt{gy}$ continuous bubble

* 2 dim. and 3 dim. mean 2 and 3 dimensional fluidized-bed

2. 3. 3. Consideration for scattering of rising velocity of continuous bubble— It was considered that the scattering of rising velocity of continuous bubble

was caused by mutual action among bubbles. Davies and Taylor's theory[4] about the bubble motion was based on that the stream of water around the the bubble was equal to the stream of fluid which was caused by solid sphere in perfect fluid and satisfied Bernoulli's theorem at the stagnant point. Applying this theory, the rising velocity of two bubbles standing side by side and one behind another could be obtained as follows.

When two spheres of radius r_{b_1} and r_{b_2} moved with the velocities $u_{b\infty_1}$ and $u_{b\infty_2}$ respectively in the perfect fluid, the approximate equation of velocity potential of the stream around the sphere was suggested by Milne-Thomson[12] when the distance l between two spheres was enough large in comparison with the size of sphere. The velocity potential ϕ_1 taking the original point of coordinate at the center of the sphere of radius r_{b_1} was shown in Eqs. (14) and (15).

When the spheres stood side by side;

$$\phi_1 = u_{b\infty_1} r\cos\theta + u_{b\infty_1}\left(\frac{r_{b_1}^3\cos\theta}{2r^2} + \frac{r_{b_1}^3 r_{b_2}^3}{4l^6} r\cos\theta\right) + u_{b\infty_2}\left(\frac{r_{b_2}^3 r\cos\theta}{2l^3} + \frac{r_{b_1}^3 r_{b_2}^3}{4l^3 r^2}\cos\theta\right) \tag{14}$$

When the spheres stood one behind another;

$$\phi_1 = u_{b\infty_1}\left\{r\cos\theta + \frac{1}{2}\frac{r_{b_1}^3\cos\theta}{r^2} + \frac{1}{2}\frac{r_{b_1}^3 r_{b_2}^3}{l^3}\left(\frac{1}{l^2} + \frac{2r\cos\theta}{l^3}\right)\right\} - u_{b\infty_2}\left\{\frac{1}{2} r_{b_2}^3\left(\frac{1}{l^2} + \frac{2r\cos\theta}{l^3}\right) + \frac{1}{2}\frac{r_{b_1}^3 r_{b_2}^3\cos\theta}{l^3 r^2}\right\} \tag{15}$$

Applying Davies and Taylor's theory to this problem, $u_{b\infty_1}$ and $u_{b\infty_2}$ could be obtained. The neat equations were obtained for $u_{b\infty_1}$.*

When two bubbles stood side be side;

$$u_{b\infty_1} = \frac{2}{3}\sqrt{g r_{b_1}}\left(1 - \sqrt{\frac{r_{b_2}}{r_{b_1}}}\frac{r_{b_2}^3}{2l^3}\right)\Big/\left(1 - \frac{r_{b_1}^3 r_{b_2}^3}{4l^6}\right) \tag{16}$$

When one behind another;

$$u_{b\infty_1} = \frac{2}{3}\sqrt{g r_{b_1}}\left(1 + \sqrt{\frac{r_{b_2}}{r_{b_1}}}\frac{r_{b_2}^3}{l^3}\right)\Big/\left(1 - \frac{r_{b_1}^3 r_{b_2}^3}{l^6}\right) \tag{17}$$

From Eqs. (16) and (17), it was deduced that the rising velocity was affected by existence of another bubble, and became smaller when the bubble stood side by side and larger when one behind another. Moreover effect of another bubble was found in the case of bubbles standing one behind another. As the actual phenomena of the bubbles in the fluidized bed were so complicated, it was doubtful whether Eq. (16) and Eq. (17) expressed the rising

* See appendix.

velocity even qualitatively but it could be explained that the rising velocity of continuous bubble scattered widely and was larger than of single bubble.

2.4. Change of state of bubble by probe

Not only the probe of capacitance method but also of light probe method which was put into the fluidized bed might change the state of fluidized bed at some degree, however small the probe was. As mentioned above the rising velocity of bubble was affected little by probe. But it should be examined whether it was appropriate or not to measure the particle contents in the bubble by these methods. When the probe was put into fluidized bed, the peak of pen-oscillograph which indicated the passing of bubble through probe did not reach the empty line as shown in Fig. 2. The same results were obtained by Yasui et al.[23] and Lanneau[11] also. Inserting probe which was as large as the one of Lanneau into two dimensional fluidized bed, the photograph was taken when the bubble passed through it. An example of it was shown in **Fig. 12.** Considerable amount of particles fell down around the probe. And also when the 0.5 mm diameter wire was installed into the fluidized bed, the same results were obtained. From these results the reason why the peak in Fig. 2 did not reach the empty line was due to the falling of particles by the probe. So it could not be deduced that there were some amount of particles in the bubble itself based on Fig. 2.

Fig. 12. Particle streaming caused by the probe when bubble passes through it.

2.5. Concentration of particles in the bubble

It was important to know how many particles were contained in the free rising bubbles. Fairly many particles fell down along the wall when the bubble rose up, so usual photography could not make clear how many particles were contained in the bubble quantitatively. For this purpose, the bubble was photographed tomographically in the two dimensional fluidized bed by the method mentioned in the section 1.2. An example of the photograph was shown in Fig. 6. Experiments were carried out with glass beads G.B. 2 at $u/u_{mf}=1.6$ (single bubble was blown into), and $u/u_{mf}=2.95$ (continuous bubble), and sand s. 2 at $u/u_{mf}=1.98$ (single bubble was blown into). The results of analysis were shown in **Table 4.** The ratio of volume occupied by particles $(1-\varepsilon)$ was at most 0.018 at wall and near the center at most 0.004. The value of $(1-\varepsilon)$ decreased as going towards the center. It is no exaggeration

Table 4. Distribution of particles $(1-\varepsilon)$ in the bubble.

particles	u/u_{fm} [−]	$1-\varepsilon$				
		place 1	place 2	place 3	place 4	place 5
G.B.2	1.60	0.0173	0.00507	0.00259	0.00461	0.0297
G.B.2	2.95	0.0164	0.00554	0.00354	0.00705	0.0128
s.2	1.98	0.00200	0.00112	0.000723	0.00110	0.00377

to say that few particles were contained at center. The reason why $(1-\varepsilon)$ was large at wall was due to the falling of particles along the wall. It was maintained in the modified two phases theory[9,10] that several % of entire particles or more were contained in the bubble, but the value obtained by the authors did not reach that value. About the concentration of particles in the bubble, the "finger" which was mentioned by Rowe[20] was not considered. The finger was recognized also from the results of X-ray photography.

Conclusion

1. The bubble rose while growing up with the process of repetion of coalescence and redispersion.
2. The bubble had the shape of spherical cap and the lower section of bubble was convex upward.
3. The rising velocities of both single and continuous bubble were proportional to the square root of vertical bubble length without relating to the kind of particles. The rising velocity of continuous bubble scattered widely and this scattering was essential.
4. There were few particles in the bubble.

Appendix

When the bubbles stood side by side, particle velocity q_1 at the surface of bubble was obtained from Eq. (14),

$$q_1^2 = \frac{9}{4} u_{b\infty_1}^2 \sin^2\theta \left(1+\frac{u_{b\infty_2}}{u_{b\infty_1}} \frac{r_{b_2}^3}{2l^3}\right)^2 \tag{A}$$

On the other hand, particle velocity q_1 was obtained from Bernoulli's theorem.

$$q_1^2 = 2gr_{b_1}(1-\cos\theta) \tag{B}$$

Equating Eq. (A) and (B) and approaching θ to zero,

$$u_{b\infty_1} = \frac{2}{3}\sqrt{gr_{b_1}} - u_{b\infty_2} \frac{r_{b_2}^3}{2l^3} \tag{C}$$

Stepping up the same process for the bubble r_{b_2}, ϕ_2 and q_2 were obtained and

$$u_{b\infty_2} = \frac{2}{3}\sqrt{gr_{b_2}} - u_{b\infty_1}\frac{r_{b_1}^3}{2l^3} \tag{D}$$

Discriminating $u_{b\infty_2}$ from Eqs. (C) and (D), Eq. (16) was obtained.

When the bubbles stood one behind another, carring out the same process,

$$q_1^2 = \frac{9}{4}u_{b\infty_1}^2 \sin^2\theta\left(1-\frac{u_{b\infty_2}}{u_{b\infty_1}}\frac{r_{b_2}^3}{l^3}\right)^2 \tag{E}$$

Equating this to Eq. (B) and approaching θ to zero,

$$u_{b\infty_1} = \frac{2}{3}\sqrt{gr_{b_1}} + u_{b\infty_2}\frac{r_{b_2}^3}{l^3} \tag{F}$$

For the bubble r_{b_2},

$$u_{b\infty_2} = \frac{2}{3}\sqrt{gr_{b_2}} + u_{b\infty_1}\frac{r_{b_2}^3}{l^3} \tag{G}$$

Discriminating $u_{b\infty_2}$ from Eqs. (F) and (G), Eq. (17) was obtained.

Nomenclature

f_b	:	fraction of bubble sphere occupied by particle wake	[—]
g	:	gravitational acceleration	[cm²/sec]
l	:	distance between bubbles	[cm]
n	:	frequency of bubbles	[no./sec]
q	:	velocity of particle at surface of bubble	[cm/sec]
r	:	radial distance of spherical coordinate	[cm]
r_b	:	radius of bubble	[cm]
t	:	time lag of channel 1 and 2 traces	[cm]
u	:	superficial velocity of fluidising fluid	[cm/sec]
u_{mf}	:	minimum fluidizing velocity	[cm/sec]
u_b	:	rising velocity of bubble	[cm/sec]
$u_{b\infty}, u_{b\infty}'$	:	rising velocity of bubble without wall effect	[cm/sec]
V_b	:	bubble volume	[cm³]
w	:	width of pen-oscillorgraph traces	[mm]
y	:	vertical length of bubble	[cm]
$\bar{y}$	:	average vertical length of bubble	[cm]
Z	:	height from distributor	[cm]
Z_c	:	settled height of bed	[cm]
ε	:	voidage fraction	[—]
θ	:	angle of spherical coordinate	[deg.]
θ_d	:	bubble angle	[deg.]
ϕ	:	velocity potential	[cm²/sec]

Literature cited

1) Baumgarten, P. K. and Pigform, R. L.: A.I. Ch. E. Journal., Vol. 6, 115 (1960).
2) Davidson, J. F., Paul, R. C., Smith, M. J. S., and Duxbury, H. A.: Trans. Instn. Chem. Engrs. (London)., Vol. 37, 323 (1959).
3) Davidson, J. F. and Harrison, D.: "Fluidised Particles" Chembridge Univ. Press. (1963).
4) Davies, R. M. and Taylor, Sir Geoffrey: Proc. Roy. Soc. (London) A, 200, 375 (1950).
5) Dotson, J. M.: A. I. Ch. E. Journal Vol. 5, 169 (1959).
6) Harrison, D., Davidson, J. F. and de. Kock, J. W.: Trans. Instn. Chem. Engrs. (London) Vol. 39, 202 (1961).
7) Harrison, D. and Leung, L. S.: Trans. Instn. Chem. Engrs. (London)., Vol. 40 146 (1962).
8) Jackson, R.: Trans. Instn. Chem. Engrs. (London) Vol. 41 13 (1963).
9) Kunii, D. and Yagi, S.: The 23rd annual meeting of Chem. Eng. Soc. of Japan April, (1958).
10) Kunii, D.: Kagakukikai Gijutsu Vol. 10 125 (1958).
11) Lanneau, K. P.: Trans. Instrn. Chem. Engrs. (London) Vol. 38, 125 (1960).
12) Milne-Thomson, L. M: Theoretical Hydrodynamics, 4th edition London; Macmillan (1960).
13) Morse, R. D. and Ballou, C. O.: Chem. Eng. Progr. Vol. 47, 199 (1951).
14) Ozaki, A. and Morikawa, K.: The 23rd annual mmeting of Chem. Eng. Soc. of Japan April (1958).
15) Reuter, H.: Chem-Ing-Tech. Vol. 35 98 (1963).
16) Reuter, H.: Chem-Ing-Tech. Vol. 35 219 (1963).
17) Rowe, P. N.: Chem. Eng. Progr. Symposium Series Vol. 58, No. 38 42 (1962).
18) Rowe, P. N. and Partrige, B. A.: Symposium of the Interaction between Fluids and Particles, 135 London Instn. Chem. Engrs. (1962).
19) Rowe, P. N. and Partridge, B. A.: Chem. Eng. Sci. Vol. 18, 511 (1963).
20) Rowe, P. N., Partridge, B. A. and Lyall, E.: United Kingdom Atomic Energy Authority Research Group Report AERE-R 4543 (1964).
21) Rowe, P. N., Partridge, B. A., Lyall, E. and Ardran, G. M.: Nature, (London) Vol. 195, 278 (1962).
22) Uno, J. and Kintner, R. C.: A. I. Ch. E. Journal, Vol. 2, 420 (1956).
23) Yasui, G. and Johanson, L. N.: A. I. Ch. E. Journal Vol. 4, 445 (1958).